Multifield direct design method for ultrashort throw ratio projection optics with two tailored mirrors

Nie, Yunfeng; Mohedano, Ruben; Benitez, Pablo; Chaves, Julio; Minano, Juan C.; Thienpont, Hugo; Duerr, Fabian

Published in:
Applied Optics

DOI:
10.1364/AO.55.003794

Publication date:
2016

applied optics

Multifield direct design method for ultrashort throw ratio projection optics with two tailored mirrors

Yunfeng Nie,[1,*] Rubén Mohedano,[2,3] Pablo Benítez,[2,3,4] Julio Chaves,[2,3] Juan C. Miñano,[2,3,4] Hugo Thienpont,[1] and Fabian Duerr[1]

[1]Brussels Photonics Team, Vrije Universiteit Brussel, Pleinlaan 2, B-1050 Brussels, Belgium
[2]Light Prescriptions Innovators, Madrid 28223, Spain
[3]Light Prescriptions Innovators, Altadena, California 91001, USA
[4]CeDint, Universidad Politecnica de Madrid, Campus de Montegancedo Pozuelo, Madrid 28223, Spain
*Corresponding author: ynie@b-phot.org

Received 11 March 2016; revised 13 April 2016; accepted 14 April 2016; posted 15 April 2016 (Doc. ID 260915); published 6 May 2016

In this work, we present a multifield direct design method for ultrashort throw ratio projection optics. The multifield design method allows us to directly calculate two freeform mirror profiles, which are fitted by odd polynomials and imported into an optical design program as an excellent starting point. Afterward, these two mirrors are represented by XY polynomial freeform surfaces for further optimization. The final configuration consists of an off-the-shelf projection lens and two XY polynomial freeform mirrors to greatly shorten the regular projection distance from 2 m to 48 cm for a 78.3 inch diagonal screen. The values of the modulation transfer function for the optimized freeform mirror system are improved to over 0.6 at 0.5 lp/mm, in comparison with its rotationally symmetric counterpart's 0.43, and the final distortion is less than 1.5%, showing a very good and well-tailored imaging performance over the entire field of view.

OCIS codes: (120.4570) Optical design of instruments; (080.4035) Mirror system design; (080.4228) Nonspherical mirror surfaces; (080.2740) Geometric optical design.

http://dx.doi.org/10.1364/AO.55.003794

1. INTRODUCTION

Short throw and ultrashort throw projectors allow large screens in very limited space, without concerns about shadows that obstruct the image or lights that shine in the presenter's face. In some specified applications such as rear projection systems [1,2], ultrashort throw distance is a prerequisite to fulfill the space constraints. A regular projector with a 1.2:1 throw ratio (TR = projection distance/screen diagonal length) would have to be 240 cm away to create an 80 in. diagonal image, while a 0.3:1 ultrashort throw ratio (TR) projector only needs 60 cm to create the same image. There are two major methods to realize the optical design of an ultrashort throw projector. The first one is to use large magnification projection objectives with three or four spherical/aspheric mirrors [3–5]. The other solution is to combine accessory optics with regular projectors as shown in Fig. 1—to name a few, the simultaneous multiple surface (SMS) optic [6–8], distortion correction optic [9–12], and field curvature correction (FCC) optic [13,14].

The SMS design method makes full usage of two skew ray bundles in different apertures to directly calculate two high-order odd polynomial surfaces, which guarantees a good mapping relationship between virtual object points created by the original projector and new image points [8]. In the distortion correction optic, it regards distortion as the most considerable aberrations in wide field of view systems such as short TR projectors; therefore one additional aspheric lens or mirror was introduced to correct distortion and then optimize other aberrations to get a good image quality [10]. With the FCC method, one additional odd polynomial mirror was added to achieve short TR. Given that one convex mirror inherently induces a curved image, the method was proposed reversely to keep a flat final image, whereas a corresponding field curvature should be reserved for the front regular projector, and an integral optimization of the whole system is required [14].

To our knowledge, all these proposed accessory optics are based on rotationally symmetric optical elements. However, the essence of the problem is to generate a tailored mapping relationship between two rectangular screens as shown in Fig. 1. The nonrotationally symmetric off-axis layout raises the question if the image quality could be further improved by using freeform mirrors. Like all optical designs, the optimization of freeform optical systems relies greatly on finding a good

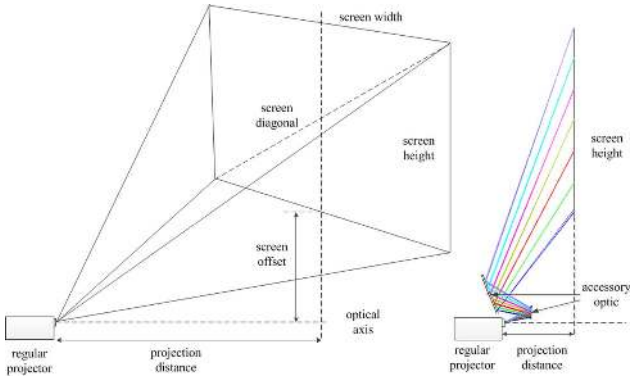

Fig. 1. Schematic drawings of a regular projector (left) and an ultrashort TR design concept by adding accessory optics (right).

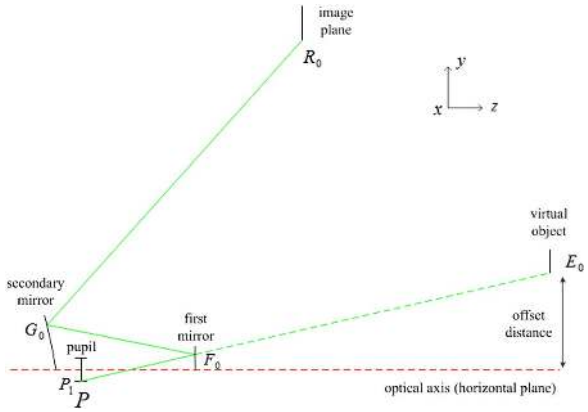

Fig. 2. Initial parameters to start the design procedures.

starting point. Several direct design methods have been developed so far to calculate freeform surfaces, such as the partially differential equations method [15–17], the SMS method for nonimaging applications [18], and a related analytic method [19]. However, either a point source or discrete fields are considered in these design algorithms with two freeform surfaces, which hinders their use in wide field of view imaging systems.

In this paper, we present a novel design method for ultrashort TR projectors based on a partial coupling of multiple fields. The procedures of how to directly calculate two off-axis freeform-profile mirrors is introduced step by step in Section 2. In Section 3, the application of this method for designing an ultrashort TR projector is illustrated, and the image quality of both rotationally symmetric aspheric mirrors and freeform mirrors is evaluated and analyzed. Finally, conclusions are drawn and the outlook is given in Section 4.

2. MULTIFIELD DIRECT DESIGN METHOD FOR TWO OFF-AXIS MIRROR IMAGING SYSTEMS

Originally, the multifield direct design method was proposed for two on-axis refractive freeform surfaces in imaging lens design with an incorporated entrance pupil [20,21]. In this work, it is further extended to solve a tailored imaging problem for an off-axis mirror system.

The initial setting is illustrated in Fig. 2. In order to avoid vignetting, the entrance pupil P is assumed to be at the exit pupil of the foregoing projector optical system. A first off-axis field E_o is constructed with a certain offset distance from the optical axis (horizontal plane). We calculate a bottom ray of field E_o from P_1 that reflects at F_0 on the first mirror, then passes by G_0 on the secondary mirror, and finally converges to point R_0 on the image plane. In most imaging systems, the ideal image points are proportional to the focal length of the optical system. However, it is noteworthy that the focal length is not used to determine the ideal image points in this design, since the focal lengths are calculated by tracing paraxial rays, which are not concerned in an off-axis system, and the improper constraint of the focal length will lead to a large distortion. Therefore, the subsequent image points are constrained with a mapping relationship defined by the magnification between virtual object point E_o and its final image R_0 instead, which ensures a low distortion system. Since the configuration consists only of mirrors, and the refractive indices for all wavelengths are the same, the system is free from chromatic aberrations.

The calculation comes from the defined first off-axis field E_o to larger fields. The complete design procedure is composed of four steps:

Step 1: The initial parameters are predefined with the specifications of the foregoing optics taken into account, including the exit pupil, the virtual object (original screen), actual image plane (tailored screen), and one point on each mirror that connects one specified ray from E_o to R_0. After these parameters are determined, the optical path length (OPL) for field E_o is calculated as

$$\mathrm{OPL}_0 = R_0G_0 + G_0F_0 - F_0E_0. \tag{1}$$

Next, we define a small initial segment F_0F_1 on the first mirror by a smooth curve, for example an even polynomial expression $z = ay^2 + b$, covering rays through half of the pupil as illustrated in Fig. 3(a). According to Fermat's principle, all the rays from one wavefront to its ideal image point have constant OPL [22]. Therefore, each ray passing through F_0F_1 from E_0 to R_0 has the same OPL, and a corresponding point and its normal on a secondary mirror is determined (for example G_1) by both Snell's law and the constant OPL condition [23]. Consequently, a segment G_0G_1 on the secondary mirror is obtained by tracing dozens of rays.

Step 2: A ray is calculated that is reflected at point F_2 on the first mirror and goes to the upper edge point G_1 on the secondary mirror, as shown in Fig. 3(b). Snell's law is applied at F_2:

$$(\overrightarrow{F_2G_1} - \overrightarrow{P_1F_2}) \times \overrightarrow{nF_2} = 0, \tag{2}$$

where $\overrightarrow{F_2G_1}$ and $\overrightarrow{P_1F_2}$ are normalized vectors; $\overrightarrow{nF_2}$ indicates the normal at point F_2 and is calculated by

$$\overrightarrow{nF_2} = (\partial z/\partial y, -1). \tag{3}$$

Solving Eqs. (2) and (3), we can get the exact position data of F_2 and its normal. After F_2 is determined, the position of virtual object point E_1 is calculated by extension of the ray P_1F_2 to the object plane. The corresponding image point R_1 for the second field E_1 is also determined by the magnification

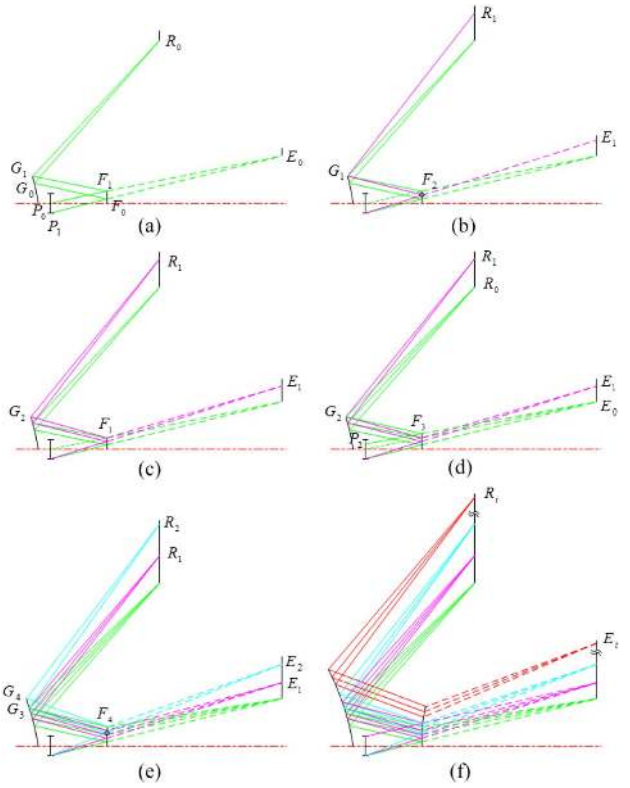

Fig. 3. Multifield design procedures to calculate two off-axis mirrors partially coupling N ($N > 3$) ray bundles: (a) Define initial segments for first field; (b) one new field is constructed by calculating a ray that passes one edge point; (c,d) calculate more points on both profiles by an iterative SMS ray tracing process; (e) another new field is constructed in analogy to the second one; (f) finalize the maximum field by interpolating known points on the first mirror and tracing rays from full aperture.

coefficient. Then, with those parameters (E_1, F_2, G_1, and R_1) known, the OPL_1 of field E_1 is calculated.

Step 3: An iterative ray tracing between fields E_0 and E_1 is executed by conducting a SMS algorithm between two adjacent fields [6]. As shown in Fig. 3(c), an edge ray from E_1 to one edge point F_1 on known segment F_0F_1 is traced, bringing in a new point G_2 on the secondary mirror by using a constant OPL_1 condition where the ray reflects to imaging point R_1. Then a new ray is calculated backward from image point R_0 to E_0, propagating already known point G_2 and leading to a new point F_3 on the first mirror with OPL_0 constant, as shown in Fig. 3(d). More rays of fields E_0 and E_1 are sampled from bottom pupil P_1 to upper pupil P_2 by repeating the procedures in Figs. 3(c) and 3(d) until reaching the pupil boundary.

Step 4: We introduce a new field E_2 by first calculating a new point F_4 on the first mirror, then obtaining its image point R_2 and OPL_2, in analogy to Step 2, as shown in Fig. 3(e). The existence of image points and OPLs for the current field E_2 and previous field E_1 allows the repetition of the design process for new sets of points on both mirrors, similar to the procedures in Step 3.

Steps 2 and 3 are repeated between two adjacent fields in each iterative ray tracing loop until the maximum field E_i is reached. To finalize the last segment for field E_i, we collect all the calculated points of the front profile and fit them into an odd polynomial curve, then extend the first profile region to allow all sampled rays covering the full pupil from E_i. Finally, the last segment of the rear profile is calculated by using the constant OPL condition. The illustrative design result is displayed in Fig. 3(f). The flow chart to calculate two off-axis tailored mirrors is shown in Fig. 4.

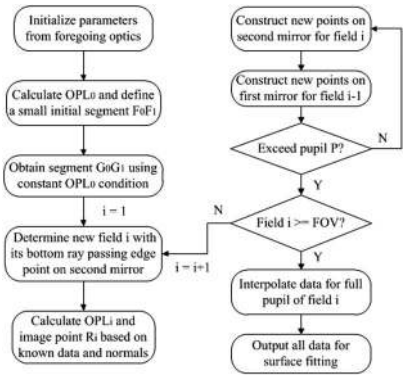

Fig. 4. Flow chart to calculate two off-axis tailored mirrors with multifield design method.

3. EXAMPLE OF DESIGNING AN ULTRASHORT THROW RATIO PROJECTOR

A. Projector Specifications and Design Procedures

We have used a commercial projector from BENQ (model MH680) as an input system, and then designed the two-mirror subsystem from its exit pupil. The specifications of this model are as follows: the TR is 1.15–1.5 (78.3 in. at 2 m), the focal length is 16.88–21.88 mm, the f-number is 2.59–2.87, and the native aspect ratio is 16:9 [24]. Many commercial projectors have similar specifications, which means that the method can be applied to other models.

The screen offset is 540 mm in the image plane. From the real object space, the height is converted to the minimum radius $r_{\min}$ of the rotationally symmetric field, which is 3 mm, as shown in Fig. 5, so the magnification coefficient is 180×.

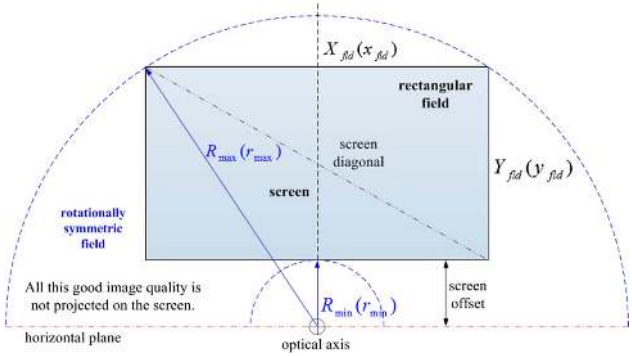

Fig. 5. Interested imaging area comparison between rotationally symmetric field design (in blue) and rectangular field design (in black). The lengths labeled in capital letters are from image space; in contrast the lowercase lengths are from the real object space.

Since the screen diagonal is supposed to be 78.3 in., the screen width X_{fld} and screen height Y_{fld} are 1728 and 972 mm, respectively. The following design and image quality are both from the perspective of object space; therefore the micro display size is calculated to be 9.6 mm in x_{fld} and 5.4 mm in y_{fld}. The maximum field for the rotationally symmetric design is therefore calculated as

$$r_{\max} = \sqrt{(r_{\min} + y_{\text{fld}})^2 + (x_{\text{fld}}/2)^2} = 9.7 \text{ mm}. \quad (4)$$

As seen from Fig. 5, in rotationally symmetric design, a two-dimensional (2D)profile that couples only tangential rays is calculated to cover the field from $r_{\min}$ to $r_{\max}$, which ensures the screen is inscribed in this annular area. Nevertheless, a majority of the good image quality that the rotationally symmetric optical system is able to offer is not projected on the screen, resulting in ineffective usage of this design's degrees of freedom. As a comparison, in the rectangular field design with two freeform mirrors incorporated, the focus area is well matched with the screen.

After all specifications are fixed (as shown in Table 1), the z coordinates for the virtual object plane ($z = 733$ mm) and the tailored screen plane ($z = 370$ mm), the magnification coefficient, and the diameter of pupil, as well as the coordinates of $F_0(19.729, 129.961)$ and $G_0(49.579, -46.997)$, are all implemented in the direct design program. We define the initial segment on the first mirror using an even polynomial expression $z = -0.0001 \times y^2 + 130$. The program stops when reaching the maximum field value 9.7 mm. It finally exports two sets of points to describe the rotationally symmetric mirrors. We first design the two accessory mirrors with the multifield direct design method in a rotationally symmetric way, then represent the two surfaces with freeform surfaces for further optimization.

B. Comparisons and Image Evaluations

1. Direct Design and Its Rotationally Symmetric Optimization Results

The two calculated profiles are fitted into odd polynomial coefficients, which we can import directly into the commercial optical design program Zemax to evaluate the results. The general expression for odd polynomial surface is given as follows [25]:

$$z(r) = \frac{cr^2}{1 + \sqrt{1 - c^2 r^2}} + \sum_i A_i r^m, \quad (5)$$

where c is the paraxial curvature of the surface, A_i is the coefficient of the polynomial terms, m is the order, and $m < 10$.

Table 1. Optical Specifications of the Ultrashort TR Projector

Parameters	Values
Micro display size (mm^2)	9.6 × 5.4
Wavelength (nm)	430–650
Magnification	180
f-number	2.6
Projection distance (cm)	48
Screen size (in.)	78.3
Throw ratio	0.24

To evaluate the modulation transfer function (MTF) performance of the design, we also need the specifications of the micro display in the projector. The MH680 projector is using a 1080p digital micromirror device (DMD). We find such an exemplary DMD for the design, the DLP4710 1080p DMD with 5.4 μm for each micromirror pitch [26]. Therefore, the cutoff spatial frequency is

$$f_{\text{cutoff}} = \frac{1000}{2 \times a} \text{ lp/mm} = 92.6 \text{ lp/mm}, \quad (6)$$

where a is the pixel size of the micro display. Given that the magnification is 180×, the cutoff spatial frequency in the screen is 0.52 lp/mm.

The MTF plots for selected fields (−3, −4, −5, −6, −7, −8, −9, and −9.7 mm in y axis) of the multifield direct design are shown in Fig. 6. From the results, the worst MTF performances are from the minimum and maximum fields. A similar phenomenon happens in the process of the surface fitting where the fitting error is relatively large in the edge part of the calculated surfaces.

Using the direct design data as a starting point, we have optimized the mirrors to reduce some fitting error as well as to improve the imaging performance. Since the design is rotationally symmetric, only half of the fields in the radial direction are optimized. The merit function is built by using the root mean square (RMS) spot radius and chief ray setting. The focal length is not controlled during the optimization process; as a substitution we have used operand REAY to make sure the mapping relationship is fulfilled and distortion is reduced to a low level by adjusting the weighting factors. All the aspheric coefficients are defined as variables during the optimization, and the design quickly converges to a well performed system within a few cycles.

The imaging performance of the optimized rotationally symmetric system is also evaluated from the perspective of MTF plots, as shown in Fig. 7. The MTF values for all the selected fields at the cutoff frequency 0.52 lp/mm are higher than 0.43. As shown in [10], where a refractive lens is added as an accessory optic, the MTF value is better than 0.6 at 0.4 lp/mm (the resolution of a DMD with 11.4 μm pixel size) for a smaller field of view. In the SMS accessory optic design [8,27], it reports a performance of MTF value better

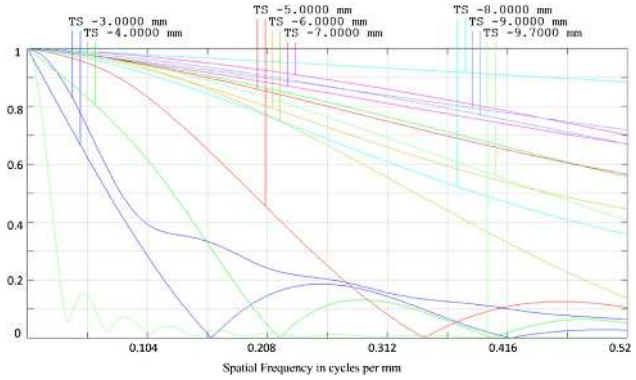

Fig. 6. MTF diagram of the multifield direct design in a rotationally symmetric system shows a good inner performance and bad edge performance.

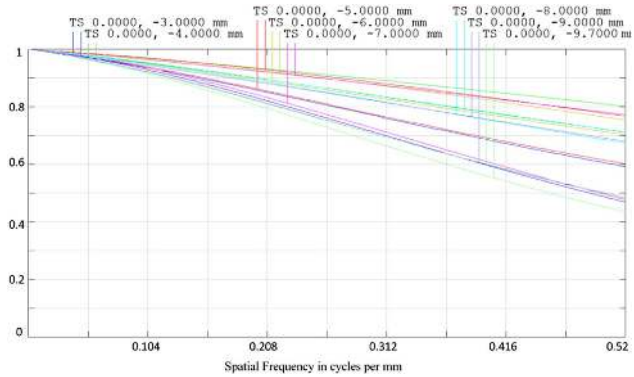

Fig. 7. MTF performance after optimization in a rotationally symmetric system is better than 0.43 at the cutoff frequency, 0.52 lp/mm.

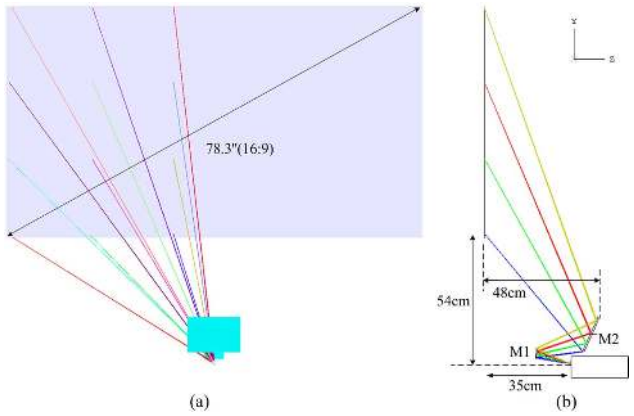

Fig. 8. 3D front view and 2D cross section layout of designed ultrashort TR projector.

than 0.61 at 0.289 lp/mm (the resolution of the standard Extended Graphics Array mode known as XGA) with the same field of view in this work. This comparison clearly demonstrates a comparable performance of our design to its counterparts of rotationally symmetric designs.

2. Optimization of Freeform Surfaces and Results

As already mentioned in Section 3.A, a rotationally symmetric design does not provide well-matched solutions for off-axis imaging systems. Since the virtue of the problem is tailoring the image from the original screen to a desired nearer screen, the freeform surfaces should be better in accomplishing the task.

The odd polynomial surfaces are refitted to XY polynomial surfaces that are described by expression

$$z(x,y) = \frac{c(x^2+y^2)}{1+\sqrt{1-c^2(x^2+y^2)}} + \sum_i A_i x^m y^n, \qquad (7)$$

where c is the paraxial curvature of the surface, A_i is the coefficient of the polynomial terms, and $m+n \le 10$. Given that the system is symmetric with respect to the y–z plane, only even x terms of each surface are not zero. Therefore, the even x terms of XY polynomial coefficients are obtained from the surface fitting program and are all imported into Zemax.

The design is further optimized with two freeform mirrors. The fields are normalized to be rectangular to better match the desired screen. Since the system is still y–z plane symmetric, only half of the fields in the $+x$ axis are taken into account. We choose 12 fields for optimization, 3 fields (−0.96, −2.88, and −4.8 mm) in the half x dimension and 4 fields (−3, −4.8, −6.6, and −8.4 mm) in the full y dimension. All the even x terms are made as variables in the optimization process, and the thicknesses are kept constant; otherwise the dimension tends to become much larger. The final layout from 3D front view and 2D profile of the ultrashort TR projector are shown in Fig. 8. The throw distance is 48 cm, projected onto a 2 m (78.3 in.) screen, so the TR is 0.24.

During the optimization, the merit function is built by evaluating the RMS spot radius over the selected fields. The chief ray of each field is selected as the reference. The focal length should not be constrained, because the problem to be solved is different from purely finding a solution for good imaging performance, but a redistribution of image with low distortion is also what we want. Therefore, we control magnification point by point, and the RMS spot radius in the default merit function will take care of the image quality. With two freeform mirrors, the system is no longer rotationally symmetric; then not only fields from one radial direction should be controlled, but also from the full rectangular aperture. We choose 4 × 5 fields that are evenly distributed in the $-x$ and full y dimensions, respectively, for distortion correction. As an off-axis imaging system, the centric y field ($y = -5.7$ mm) is selected as the reference field for correcting distortion, and the position of its image point is $(X_{\text{ref}}, Y_{\text{ref}})$. For one specified field, the ideal position in the image plane is $(X_{\text{ideal}}, Y_{\text{ideal}})$ when the real position is $(X_{\text{real}}, Y_{\text{real}})$; then the distortion is defined as

$$\text{distortion} = \frac{\sqrt{(X_{\text{real}}-X_{\text{ideal}})^2+(Y_{\text{real}}-Y_{\text{ideal}})^2}}{\sqrt{(X_{\text{real}}-X_{\text{ref}})^2+(Y_{\text{real}}-Y_{\text{ref}})^2}} \times 100\%. \qquad (8)$$

The distortion for each field is then added in the final merit function, and the weighting factor is properly assigned during the optimization. At the beginning, if other aberrations are possessing a relatively high contribution percentage, a high value of weighting factor for distortion is preferred; otherwise, a small weight is recommended and is better for improving the image quality.

After optimization, the design quickly converges to a well-balanced result. The obtained distortion grid is shown in Fig. 9. The red solid grid indicates the ideal image without distortion, and the black dashed grid is plotted by real ray tracing. The aspect ratio of the figure is 16:9, the same as that of the screen. From the result, the distortion is corrected quite well, and the maximum absolute value is lower than 1.5%.

Figure 10 shows the image quality from the perspective of MTF values over the 12 equidistance defined fields. The maximum field (−4.8, −8.4) mm is the same as the maximum radius in the rotationally symmetric design when converted to the radial value. As shown in the figure, the MTF performance is higher than 0.58 at the cutoff frequency, 0.52 lp/mm, after optimization with two freeform mirrors, much better than the

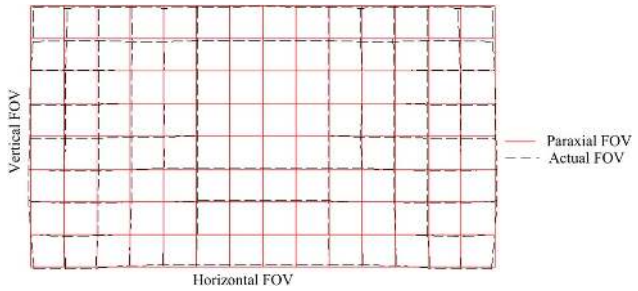

Fig. 9. Maximum distortion of the design with two freeform mirrors is below 1.5% with respect to a 16:9 rectangular screen.

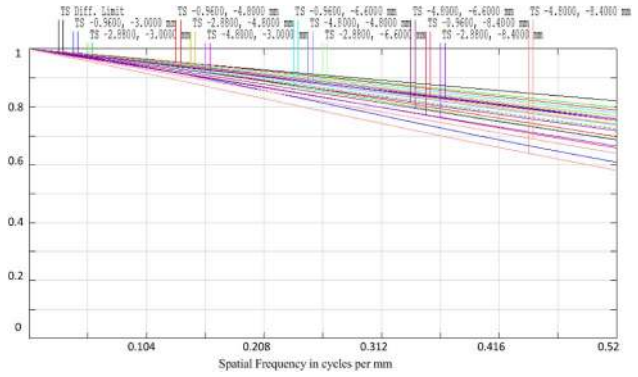

Fig. 10. MTF performance after optimization with two freeform mirrors is higher than 0.58 at the cutoff frequency, 0.52 lp/mm.

rotationally symmetric designs targeting the same specifications. It clearly highlights the potential use of freeform optics in increasing off-axis imaging performance and/or solving a tailored imaging problem, where the field of view to be designed is far from being circularly symmetric. The RMS spot radii range from 0.161 to 0.389 mm over the full field of view, as shown in Fig. 11. The added black circles in the spot diagrams correspond to the Airy disk diameters, which are

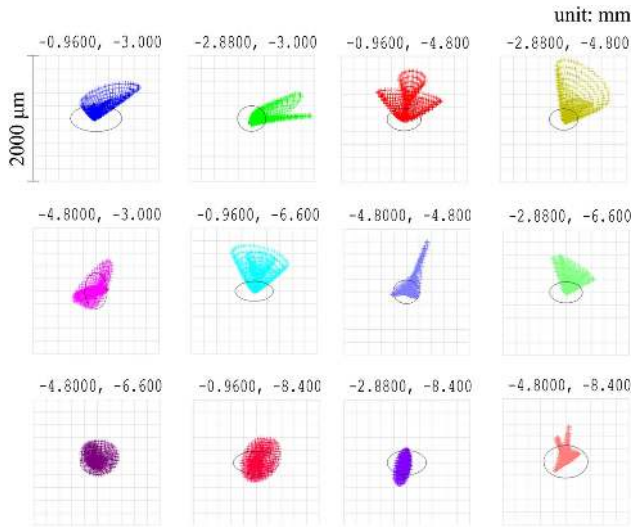

Fig. 11. RMS spot diagrams after optimization with two freeform mirrors show a well-balanced imaging performance.

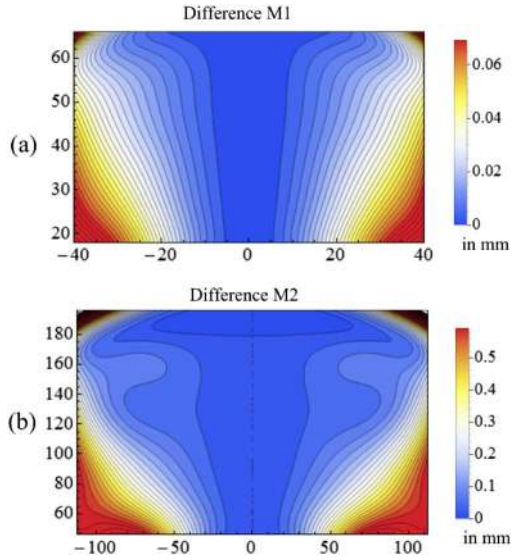

Fig. 12. Contour plots of (a) the first mirror and (b) the secondary mirror, where the optimized rotationally symmetric bases have been subtracted from the optimized freeform mirrors.

determined by real ray tracing at the reference wavelength and f-number.

To distinguish the deviations of the freeform mirrors from their rotationally symmetric counterparts, Fig. 12 shows the surface contour plots of the first and secondary mirrors where the optimized rotationally symmetric bases have been subtracted from the freeform mirrors. In the first mirror, the maximum deviation is about 0.06 mm, while in the second mirror the maximum deviation is about 0.5 mm, and they are both in the border part of the mirrors, clearly displaying a nonrotationally symmetric surface sag.

4. CONCLUSIONS

The multifield direct design method has already shown its potential in designing on-axis freeform imaging systems. In this work, we present its application in designing an ultrashort TR projector with an off-axis mirror subsystem. The final optical system of the projector consists of an off-the-shelf refractive optical lens and two accessory freeform mirrors, which greatly shortens the throw distance from 2 m to 48 cm for a 78.3 in. screen while obtaining a low-distortion and well-balanced imaging quality.

The essence of designing an ultrashort TR projector by adding an off-axis accessory optic is pursuing both good imaging quality and tailored rectangular imaging distribution where the situation is somewhat similar to nonimaging optics. Hence, freeform optics are key to achieving an effective and well-matched rectangular imaging distribution without the mismatched image quality the rotationally symmetric systems do offer.

The presented multifield direct design method has demonstrated that it can provide a good starting point for further optimization of such freeform optical systems. In terms of MTF values, the developed freeform mirror system clearly outperforms its rotationally symmetric counterpart while keeping all other specifications the same.

Funding. People Programme (Marie Curie Actions) of the European Union's Seventh Framework Programme (FP7) (2007-2013) (PITN-GA-2013-608082 (ADOPSYS)); Research Foundation–Flanders (FWO-Vlaanderen); Interuniversity Attraction Poles of the Belgian Science Policy Office (IAPBELSPO) (IAP P7-35 photonics@be), Industrial Research Funding (IOF), Methusalem; Onderzoeksraad (OZR) of the Vrije Universiteit Brussel.

Acknowledgment. We thank Vrije Universiteit Brussel and Light Prescriptions Innovators LLC for providing necessary equipment.

REFERENCES

1. M. Kuwata, T. Sasagawa, K. Kojima, J. Aizawa, A. Miyata, S. Shikama, and H. Sugiura, "Projection optical system for a compact rear projector," J. Soc. Inf. Disp. **14**, 199–206 (2006).
2. S. Shikama, H. Suzuki, and K. Teramoto, "Optical system of ultra-thin rear projector equipped with refractive-reflective projection optics," SID Symp. Dig. Tech. Pap. **33**, 1250–1253 (2002).
3. J. Ogawa, "Reflection type image forming optical system and projector," U.S. patent 6,612,704 (2 September 2003).
4. J. Ogawa, K. Agata, M. Sakamoto, K. Urano, and T. Matsumoto, "Super-short-focus front projector with aspheric-mirror projection optical system," J. Soc. Inf. Disp. **13**, 111–116 (2005).
5. Z. Zheng, X. Sun, X. Liu, and P. Gu, "Design of reflective projection lens with Zernike polynomials surfaces," Displays **29**, 412–417 (2008).
6. J. C. Minano, P. Benitez, W. Lin, J. Infante, F. Munoz, and A. Santamaria, "An application of the SMS method for imaging designs," Opt. Express **17**, 24036–24044 (2009).
7. J. C. Miñano, P. Benítez, and F. Muñoz, "Imaging optics designed by the simultaneous multiple surface method," U.S. patent 8,035,898 (11 October 2011).
8. F. Muñoz, P. Benítez, and J. C. Miñano, "High-order aspherics: the SMS nonimaging design method applied to imaging optics," Proc. SPIE **7100**, 71000K (2008).
9. Z. S. Bassi, G. L. Smith, and L. Lee, "Short throw projection system and method," U.S. patent 7,239,360 (3 July 2007).
10. Y. Bian, H. Li, Y. Wang, Z. Zheng, and X. Liu, "Method to design two aspheric surfaces for a wide field of view imaging system with low distortion," Appl. Opt. **54**, 8241–8247 (2015).
11. R. A. Hicks and R. Bajcsy, "Catadioptric sensors that approximate wide-angle perspective projections," in *Proceedings of IEEE Conference on Computer Vision and Pattern Recognition* (IEEE, 2000), pp. 545–551.
12. J. Hou, H. Li, R. Wu, P. Liu, Z. Zheng, and X. Liu, "Method to design two aspheric surfaces for imaging system," Appl. Opt. **52**, 2294 (2013).
13. M. Kuwata and T. Sasagawa, "Projection optical system and image display apparatus," U.S. patent 8,337,024 (25 December 2012).
14. Z. Zhuang, Y. Chen, F. Yu, and X. Sun, "Field curvature correction method for ultrashort throw ratio projection optics design using an odd polynomial mirror surface," Appl. Opt. **53**, E69–E76 (2014).
15. R. A. Hicks, "Direct methods for freeform surface design," Proc. SPIE **6668**, 666802 (2007).
16. D. Cheng, Y. Wang, and H. Hua, "Free form optical system design with differential equations," Proc. SPIE **7849**, 78490Q (2010).
17. H. Ries and J. Muschaweck, "Tailored freeform optical surfaces," J. Opt. Soc. Am. A **19**, 590–595 (2002).
18. P. Benítez, J. C. Miñano, J. Blen, R. N. Mohedano, J. L. Chaves, O. Dross, M. Hernandez, and W. Falicoff, "Simultaneous multiple surface optical design method in three dimensions," Opt. Eng. **43**, 1489–1502 (2004).
19. F. Duerr, P. Benítez, J. C. Miñano, Y. Meuret, and H. Thienpont, "Analytic design method for optimal imaging: coupling three ray sets using two free-form lens profiles," Opt. Express **20**, 5576–5585 (2012).
20. Y. Nie, H. Thienpont, and F. Duerr, "Multi-fields direct design approach in 3D: calculating a two-surface freeform lens with an entrance pupil for line imaging systems," Opt. Express **23**, 34042–34054 (2015).
21. Y. Nie, F. Duerr, and H. Thienpont, "Direct design approach to calculate a two-surface lens with an entrance pupil for application in wide field-of-view imaging," Opt. Eng. **54**, 15102–15108 (2015).
22. M. Born and E. Wolf, *Principles of Optics*, 7th ed. (Cambridge University, 1999).
23. J. Chaves, *Introduction to Nonimaging Optics* (CRC Press, 2008).
24. http://www.benq.com/product/projector/MH680/specifications/.
25. Zemax Manual (Zemax LLC, 2014).
26. http://www.ti.com/product/dlp4710.
27. F. Muñoz, *Sistemas Opticos Avanzados De Gran Compactibilidad Con Aplicaciones En Formacion De Imagen y En Iluminacion* (Universidad Politécnica de Madrid, 2004).